

Training in polarization through a virtual learning environment

A. Lizana^a, M. J. Yzuel^a, J.C. Escalera^a, and J. Campos*^a

^aDept. de Física, Universitat Autònoma de Barcelona, Bellaterra 08193, SPAIN

ABSTRACT

In this work, we describe the use of a virtual learning environment that we have developed. The software is programmed in LabView code and it is devised to teach polarization concepts to students in Optics courses at the university, either at the degree or master levels.

In order to consolidate the knowledge previously explained in theoretical and experimental courses, the applet tries to foster the interaction of students with different virtual environments, each one training one particular polarization feature or method. In particular, the following concepts are included in the applet: ellipse of polarization, Poincaré sphere, Stokes vectors, Mueller matrix transformations, and polarization dependence with light wavelength after material interaction.

What is more, we perform a set of targeted questions to students, into a problem-solving approach. It consists of a series of brief questions that students must solve and answer, helped by the visual information they can find into the applet. In this way, some theoretical concepts related to polarization are thought and reviewed by students from a different perspective from that given in the theoretical classes at the classroom.

Keywords: Polarization, Polarimetry, Stokes vector, Mueller matrices, Poincaré sphere, Lyot filter, Solc filter

1. INTRODUCTION

Polarization is an inherent property of transversal waves. In the case of electromagnetic waves, as light beams, it describes the oscillation direction of electromagnetic fields¹. Polarization of light, degree of polarization, and modifications of light polarization after interaction with materials, provide important information of light beams and materials. For this reason, polarimetry, being the measurement and interpretation of the polarization of transverse waves or of the polarimetric transfer function of materials, is widely used in a large number of applications, as for instance, for the characterization of the optical parameters (index of refraction, thickness, absorption coefficient, roughness, etc.) of materials structured in thin films²⁻⁵, in remote sensing⁶, applications in astronomy^{7,8}, for medical applications^{9,10}, in biophotonics¹¹⁻¹⁶, among many others.

Due to the significance of polarimetry in science and technology, a thorough polarization background gives access to a wide variety of career opportunities. In order to train students in this topic, polarization studies are included in many academic curriculums in the areas of sciences and engineering, either at the degree or master levels. The most used training approach consists of providing theoretical lectures, where some polarization fundamentals are provided, and in some cases, to accompany and reinforce this theoretical information by means of a series of experimental sessions. These theoretical and experimental sessions are given either as different blocks into the same course, or as independent and complementary subjects, depending on the particular academic curriculums. Note that experimental sessions are highly recommended for a deep learning of the theoretical concepts previously provided, as they are revised from a different point of view, but they are not always accessible in all the educational institutions, and thus, experimental approaches may not be present in many academic curriculums.

In last decades, the use of interactive applets as supporting tools for the training of multiple academic disciplines is increasing in number. This situation is clear by checking the number of Java (Matlab, LabView, etc.) applets used for the creation of interactive labs for topics in Mathematics, Physical Sciences and Technology, that can be easily found as academic resources provided by universities, technological institutes, enterprises, educational blogs of academic and technical individuals, etc. According to this tendency, we have developed a polarization-based applet to be used as a framework for polarization training and as a complement to theoretical and experimental sessions. The developed applet provides some polarization background in a virtual environment programmed in LabView, and the included resources aims to foster the user-applet interaction. We have built up the applet so that the concepts that it includes are complementary to the polarization block of the Optics course taught at the third year of the Physics degree in the

Universitat Autònoma de Barcelona (UAB), and it is suitable for students at university degree and master degree levels. In particular, the polarization concepts included in the applet are: ellipse of polarization, Poincaré sphere, Stokes vectors, Mueller matrix transformations, polarization dependence with light wavelength after material interaction and polarization filters.

The outline of this paper is as follows. In section 2 we provide the theoretical foundations related to the different polarization concepts taught and the tools included in the polarization applet. In section 3, we describe different aspects of the virtual environment of the polarization applet, detailing the different educational utilities, calculation tools and visual representations present in the software. The applet is organized in different tabs where some particular polarization concepts are gathered, so this section is arranged in different subsections providing the structure of the applet. In section 4, we describe the educational approach we have conducted to train polarization concepts through the polarization applet. Finally, the main conclusions of the work are provided in section 5.

2. POLARIZATION FOUNDATIONS

In this section, we briefly provide the definitions and mathematical descriptions of some polarization concepts included in the developed polarization-based applet.

2.1 Ellipse of polarization, Stokes vectors and Poincaré representation

The main polarization theoretical concepts included in the polarization applet are following described.

2.1.1 Ellipse of polarization

Let us write the two electrical field orthogonal components of a plane wave propagating in the positive direction of the z axis,

$$E_x(z, t) = A_x \cos(\omega t - kz) \quad (1a)$$

$$E_y(z, t) = A_y \cos(\omega t - kz + \varphi) \quad (1b)$$

where ω is the angular frequency of light, $k = \frac{2\pi}{\lambda}$ is the wavenumber (where λ is the light wavelength) and

$\varphi = \varphi_y - \varphi_x$ is the initial phase difference between the E_x and E_y orthogonal plane waves.

Starting from Eqs. (1) we can study the trajectory described by the electrical field as a function of time. By setting $z=0$ in Eqs. (1) and expanding the argument cosine by using trigonometric relations we obtain,

$$\frac{E_x(t)}{A_x} = \cos(\omega t) \quad (2a)$$

$$\frac{E_y(t)}{A_y} = \cos(\omega t) \cos(\varphi) - \sin(\omega t) \sin(\varphi) \quad (2b)$$

Replacing Eq. (2a) in (2b) and squaring the resulting relation leads to,

$$\frac{E_x^2(t)}{A_x^2} \cos^2(\varphi) + \frac{E_y^2(t)}{A_y^2} - 2 \frac{E_x(t)}{A_x} \frac{E_y(t)}{A_y} \cos(\varphi) = \sin^2(\omega t) \sin^2(\varphi) \quad (3)$$

Afterwards, multiplying Eq. (1b) by the factor $\sin(\varphi)$, for $z=0$, and squaring,

$$\left(\frac{E_x(t)}{A_x} \right)^2 \sin^2(\varphi) = \cos^2(\omega t) \sin^2(\varphi) \quad (4)$$

Finally, by adding Eqs. (3) and (4) we obtain,

$$\frac{E_x^2(t)}{A_x^2} + \frac{E_y^2(t)}{A_y^2} - 2 \frac{E_x(t)}{A_x} \frac{E_y(t)}{A_y} \cos(\varphi) = \sin^2(\varphi) \quad (5)$$

Note that Eq. (5) is the equation of an ellipse, meaning that the electric field temporal evolution describes an ellipse called polarization ellipse, whose characteristic parameters completely describes the state of polarization of a fully polarized beam. A representation of the polarization ellipse is given in Fig. 1(a), where it is plotted inscribed into the rectangle defined by the orthogonal basis set by its constituent electric fields E_x and E_y . In this basis, the polarization is fully described by knowing the amplitudes A_x , A_y and the retardance φ between components.

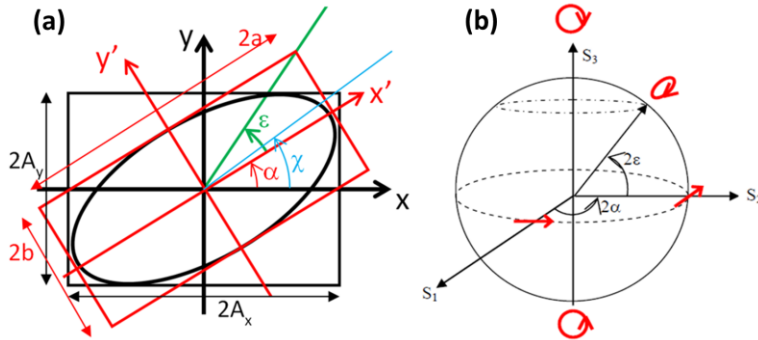


Figure 1. (a) Ellipse of polarization; and (b) Poincaré sphere.

To evaluate what is the sense of rotation of the electric field $\vec{E}(z,t)$ we can do the following analysis. By taking into account Eqs. (1), for $t=0$ and at the plane $z=0$, the electric field components take the values,

$$E_x|_{t=z=0} = A_x \quad (6a)$$

$$E_y|_{t=z=0} = A_y \cos(\varphi) \quad (6b)$$

Deriving the y -component of the field in Eq. (1b) as a function of time, for $z=0$, and evaluating it at $t=0$, permits us to study the evolution of the electric field. We obtain,

$$\left. \frac{\partial E_y}{\partial t} \right|_{t=0} = -A_y \omega \sin(\varphi) \quad (7)$$

From Eq. (7) we see how E_y is decreasing into the interval $0 < \varphi < \pi$, this leading to right-handed polarization into this range, whereas E_y is growing in the interval $\pi < \varphi < 2\pi$, this leading to left-handed polarization into this range. Note that the criterion we used is the following: right-handed for light coming to the observer rotating clockwise and left-handed for light coming to the observer rotating counterclockwise.

By performing a coordinate system rotation, we can describe the polarization ellipse from the basis of its main axes (the major semi-axis and the minor semi-axis). It is illustrated in Fig. 1(a) with the x' and y' axes in red, which are rotated an angle α (called azimuth angle) with respect to the x - y basis. Another angle of interest is the so called ellipticity angle ε (green angle in Fig. 1(a)), which is defined as the ratio between the semi-minor and the semi-major axes of the polarization ellipse. This angle can be geometrically understood as the angle between the x' axis and the diagonal of the rectangle in which the ellipse of polarization is inserted according its own axes (see Fig. 1(a)). As its name suggests, it provides the ellipticity of the polarization ellipse, which ranges from 0, for linear polarization, to $\pm\pi/4$, for circular polarization. Importantly, by knowing the azimuth α and ellipticity ε angles, the polarization of a fully polarized beam is fully determined.

The relations between the amplitudes (A_x , A_y) and phase φ polarization description space, and the azimuth and ellipticity (α , ε ; polarization angles) space are given below¹⁷:

$$\tan 2\alpha = \frac{2A_x A_y}{A_x^2 - A_y^2} \cos \varphi = \tan 2\chi \cos \varphi \quad (8)$$

$$\tan 2\varepsilon = -q \sin 2\alpha \tan \varphi \quad (9)$$

where $\tan \chi = \frac{A_y}{A_x}$ and $q = \pm 1$ (with minus sign, $-$, for right-handed and plus sign, $+$, for left-handed).

2.1.2 Stokes vectors and Poincaré sphere

Another way to describe the polarization of a light beam is by using the so called Stokes vector¹⁷, which comprises four intensity magnitudes, the Stokes parameters, arranged in column format. The Stokes vector parameters can be calculated from the magnitudes of the polarization ellipse described in section 2.1.1, but unlike the polarization ellipse, Stokes vectors are able to describe partially polarized or fully depolarized beams. The normalized Stokes vector (i.e., normalized by the S_0 channel) as a function of the ellipse of polarization magnitudes in its different bases is given below,

$$S = \begin{pmatrix} S_0 \\ S_1 \\ S_2 \\ S_3 \end{pmatrix} = \frac{1}{A_x^2 + A_y^2} \begin{pmatrix} A_x^2 + A_y^2 \\ A_x^2 - A_y^2 \\ 2A_x A_y \cos \varphi \\ 2A_x A_y \sin \varphi \end{pmatrix} = \begin{pmatrix} 1 \\ \cos 2\chi \\ \sin 2\chi \cos \varphi \\ \sin 2\chi \sin \varphi \end{pmatrix} = \begin{pmatrix} 1 \\ \cos 2\varepsilon \cos 2\alpha \\ \cos 2\varepsilon \sin 2\alpha \\ \sin 2\varepsilon \end{pmatrix} \quad (10)$$

Each parameter in the Stokes vector provides particular information of the analyzed state of polarization (SoP). The S_0 parameter is the intensity of the analyzed light; the S_1 parameter estimates the contribution of linear polarization in the horizontal or vertical directions; the S_2 parameter estimates the contribution of linear polarization at 45 or at 135 degrees from the vertical; and the S_3 parameter provides the contribution of circular polarization light of the studied SoP.

As stated before, Stokes vectors are appropriate to describe partial polarized and fully depolarized beam. The Degree of Polarization (*DoP*) of the studied beam can be calculated as the ratio between the fully polarized content over the total intensity, as follows¹⁷,

$$DoP = \frac{\sqrt{S_1^2 + S_2^2 + S_3^2}}{S_0} \quad (11)$$

where $0 \leq DoP \leq 1$.

Sometimes, it is interesting to study the fully polarized and the unpolarized contributions separately. It can be done by decomposing the Stokes vector in Eq. (10) as the addition of two different contributions,

$$S = S_{unpolarized} + S_{polarized} = \begin{pmatrix} S_0 - \sqrt{S_1^2 + S_2^2 + S_3^2} \\ 0 \\ 0 \\ 0 \end{pmatrix} + \begin{pmatrix} \sqrt{S_1^2 + S_2^2 + S_3^2} \\ S_1 \\ S_2 \\ S_3 \end{pmatrix} \quad (12)$$

A very useful tool to visualize SoPs into a three-dimensional space is the so called Poincaré sphere¹⁷ (see Fig. 1(b)). The fully polarized SoPs are represented over the surface of the Poincaré sphere of radius $\sqrt{S_1^2 + S_2^2 + S_3^2}$ and each two orthogonal polarizations are located at two diametrically opposed spots over the sphere. The linear polarizations are located at the equator of the sphere, completing a rotation of 180 degrees along the equator. The circular polarizations are located at the poles of the sphere (North Pole for right-handed polarization and South Pole for left-handed polarization). Any other point over the Poincaré sphere is related with an elliptical polarization, this being specified by its ellipticity angle ε (see Fig. 1(b)). By contrast, points located inside the sphere describes partial polarized SoPs, the sphere center corresponding to a state of polarization fully unpolarized.

2.2 Mueller matrices

The Mueller matrices can be understood as the transfer function of polarimetric systems. They are 4x4 matrices of real entries that encode the polarimetric properties of materials (diattenuation, retardance and depolarization), and relate the input (S) and output (S') states of polarization by means of the following linear relation¹⁷,

$$S' = \begin{pmatrix} m_{00} & m_{01} & m_{02} & m_{03} \\ m_{10} & m_{11} & m_{12} & m_{13} \\ m_{20} & m_{21} & m_{22} & m_{23} \\ m_{30} & m_{31} & m_{32} & m_{33} \end{pmatrix} S = MS \quad (13)$$

To describe a polarizing sample with its axis rotated to an angle θ from the laboratory vertical, for instance, to describe a polarizer with its transmission axis rotated or a linear retarder with its neutral line rotated, the following rotations are applied¹⁷,

$$M|_{\theta} = M_{ROT}(-2\theta)M|_{0^\circ}M_{ROT}(2\theta) \quad (14)$$

where $M|_{0^\circ}$ is the Mueller matrix of the sample without rotation (i.e., at 0 degrees of the laboratory vertical), and M_{ROT} is the Mueller matrix of a rotator that is given by,

$$M_{ROT}(\theta) = \begin{pmatrix} 1 & \cos 2\theta & \sin 2\theta & 0 \\ \cos 2\theta & \cos^2 2\theta & \cos 2\theta \sin 2\theta & 0 \\ \sin 2\theta & \cos 2\theta \sin 2\theta & \sin^2 2\theta & 0 \\ 0 & 0 & 0 & 0 \end{pmatrix} \quad (15)$$

As each Mueller matrix represents the interaction of an input polarization with a media, when light is transmitted (reflected or scattered) through different medias, i.e. when dealing with a cascade of polarization materials, the polarization of light exiting from such complex system is calculated as the product of the Mueller matrices of all the corresponding elements, from right to left, i.e.,

$$S' = (M_N \dots M_2 M_1) S \quad (16)$$

where each matrix M_i in the product can be rotated according to Eq. (14).

2.3 Polarization dependence with light wavelength after material interaction and polarization filters

In order to produce a narrow passband of transmitted wavelengths in the visible range, and thus, to build color filters, polarizing structures can be used, which usually consist of customized cascades of polarizing elements. Two well-known optical filters based on birefringence are the Lyot filter¹⁸ and the Solc filter^{19,20}. We focus in these two particular schemes as they are implemented in the applet. As the Stokes-Mueller formalism has been briefly described in sections 2.1 and 2.2, it is also used to describe the stated filters in the following.

2.3.1 Lyot filter

The main structure of a Lyot filter is sketched in Fig. 2(a). It consists of a series of N optical blocks where each block is composed of a uniaxial anisotropic plate inserted between two polarizers. On this basis, different versions of the Lyot filter have been proposed in literature^{18,19}. In the so called Lyot filter type II^{18,19}, the thickness of each successive plate in the Lyot filter is half that of the preceding. Transmission axes of polarizers are parallel between them and neutral lines of plates are also parallel between them. However, transmission axes are oriented at 45° with respect to neutral lines.

The intensity at the exit of a Lyot filter can be modeled by using the Stokes-Mueller formalism. Let us suppose that polarizers are oriented at 45° of the laboratory vertical, and anisotropic plates are oriented at 0° of the lab. vertical. Under such scenario, the intensity at the exit of the filter is given by,

$$\begin{aligned}
I(\lambda) \Big|_{L_{tot}} &= S_{LP45^\circ}^T \cdots M_{LP45^\circ} M_{R0^\circ} S_{LP45^\circ} = \\
&= \frac{E_0^2}{2(N+1)} (1 \ 0 \ 1 \ 0) \cdots \underbrace{\left(\begin{array}{cccc} 1 & 0 & 0 & 0 \\ 0 & 1 & 0 & 0 \\ 0 & 0 & 0 & 0 \\ 1 & 0 & 1 & 0 \\ 0 & 0 & 0 & 0 \end{array} \right)}_{N-2 \text{ BLOCKS}} \underbrace{\left(\begin{array}{cccc} 1 & 0 & 0 & 0 \\ 0 & 0 & 0 & 0 \\ 0 & 0 & \cos \frac{\delta}{2} & \sin \frac{\delta}{2} \\ 0 & 0 & -\sin \frac{\delta}{2} & \cos \frac{\delta}{2} \end{array} \right)}_{\text{BLOCK 2}} \underbrace{\left(\begin{array}{cccc} 1 & 0 & 1 & 0 \\ 0 & 0 & 0 & 0 \\ 1 & 0 & 1 & 0 \\ 0 & 0 & 0 & 0 \end{array} \right)}_{\text{BLOCK 1}} \underbrace{\left(\begin{array}{cccc} 1 & 0 & 0 & 0 \\ 0 & 1 & 0 & 0 \\ 0 & 0 & \cos \delta & \sin \delta \\ 0 & 0 & -\sin \delta & \cos \delta \end{array} \right)}_{\left(\begin{array}{c} 1 \\ 0 \\ 0 \\ 1 \end{array} \right)} \left(\begin{array}{c} 1 \\ 0 \\ 0 \\ 0 \end{array} \right)
\end{aligned} \tag{17}$$

where E_0 is the amplitude the incident field, S_{LP45° is the Stokes vector of a linear polarization at 45° of the lab vertical, M_{R0° is the Mueller matrix of a retarder oriented at 0° of the laboratory vertical and with retardance $\delta = \frac{2\pi}{\lambda} (n_e - n_o) d$, n_e and n_o being the extraordinary and ordinary indices of the anisotropic crystal and d its thickness.

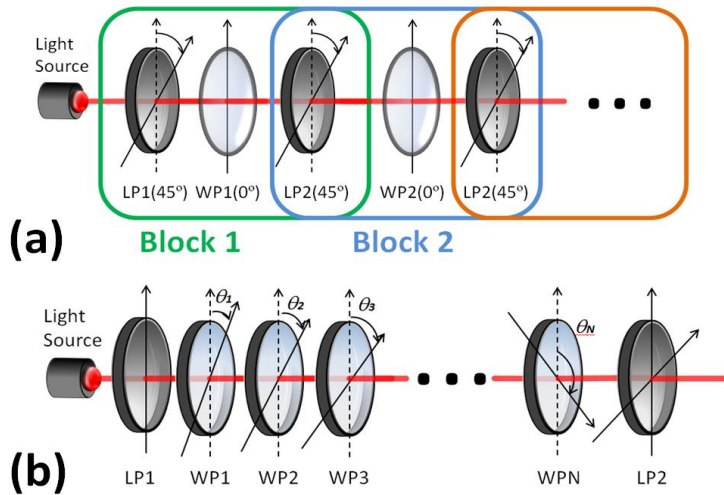


Figure 2. Optical filter sketch: (a) Lyot filter; and (b) Solc filter.

Equation (17) leads to,

$$I(\lambda) = E_0^2 \prod_{i=1}^N \cos^2 \left(\frac{\delta(\lambda)}{2^i} \right) \tag{18}$$

where E_0 is the amplitude of the incident field and $\delta(\lambda)$ is the retardance of the first plate.

The largest stage sets the bandwidth and the smallest stage sets the Free Spectral Range. If you use two of the second largest crystals, it will increase the contrast of the desired line. If you split the crystals in half and add a 1/2 waveplates in the middle you can increase the field of view of the filter. The separation and narrowness of the transmission peaks depends on the number, thicknesses, and orientation of the plates.

2.3.2 Solc filter

Another birefringent filter, composed of a series of retardation plates between a single pair of polarizers, was described by Solc¹⁹. Two main variants of this filter exist. In the fan configuration the two polarizers are parallel to one another and the i th plate is inclined to an angle $\theta_i = (i - 0.5)\pi/2N$ to them. By contrast, the polarizers in the folded configuration are crossed, and the i th plate makes an angle of $\theta_i = (-1)^i \pi/4N$ with respect to the first polarizer. Beyond these main Solc schemes, some authors have studied other configurations (different angular functions among plates or number of plates) to analyze their influence with the final filter efficiency²¹. A sketch of a possible configuration for the Solc filter is shown in Fig. 2(b).

It has been shown that the Solc filter is inferior to the Lyot filter in the suppression of parasitic light in secondary maxima near the primary transmission bands, although its band width is slightly less, and its transparency is very much better than Lyot filters²⁰. In fact, a greatest advantage of this filter over the Lyot filter is that only two polarizers are required for an efficient performance of the filter, this leading to far less light losses.

The intensity at the exit of the Solc filter shown in Fig. 2(b) can be modeled by using the Stokes-Mueller formalism. Let us suppose that the polarizers at the entrance and exit of the retardation plates are oriented at 0° of the laboratory vertical (fan configuration), and that the orientation of the N anisotropic plates progressively increase starting from 0°. In this case, the intensity at the exit of the filter is given by,

$$I(\lambda)|_{\text{Solc}} = S_{LPO}^T M_{R\theta N} \cdots M_{R\theta 2} M_{R\theta 1} S_{LPO} = \\ = \frac{E_0^2}{4} (1 \ 1 \ 0 \ 0) \begin{pmatrix} 1 & 0 & 0 & 0 \\ 0 & \cos^2 2\theta_N + \cos \delta \sin^2 2\theta_N & (1-\cos \delta) \sin 2\theta_N \cos 2\theta_N & -\sin \delta \sin 2\theta_N \\ 0 & (1-\cos \delta) \sin 2\theta_N \cos 2\theta_N & \sin^2 2\theta_N + \cos \delta \cos^2 2\theta_N & \sin \delta \cos 2\theta_N \\ 0 & \sin \delta \sin 2\theta_N & -\sin \delta \cos 2\theta_N & \cos \delta \end{pmatrix} \cdots \begin{pmatrix} 1 & 0 & 0 & 0 \\ 0 & \cos^2 2\theta_i + \cos \delta \sin^2 2\theta_i & (1-\cos \delta) \sin 2\theta_i \cos 2\theta_i & -\sin \delta \sin 2\theta_i \\ 0 & (1-\cos \delta) \sin 2\theta_i \cos 2\theta_i & \sin^2 2\theta_i + \cos \delta \cos^2 2\theta_i & \sin \delta \cos 2\theta_i \\ 0 & \sin \delta \sin 2\theta_i & -\sin \delta \cos 2\theta_i & \cos \delta \end{pmatrix} \begin{pmatrix} 1 \\ 1 \\ 1 \\ 1 \end{pmatrix} \\ (19)$$

where E_0 is the amplitude of the incident field, θ_i is the orientation angle of each anisotropic plate, and $\delta(\lambda)$ is the retardance selected for the plates.

2.3.3. Optical filters and human eye perception

The optical filters described in sections 2.3.1 and 2.3.2 lead to certain intensity distributions as a function of the wavelength. However, the final color observed by users of these filters will be affected by the spectral distribution of the source illuminating the filter, and the spectral sensitivity function of the detector.

The three color sensitivities of the human eye (cones sensitivities) must be considered if light exiting from the filter is observed to the naked eye. The Commission Internationale de l'Eclairage (CIE) 1931 color spaces were the first quantitative relations defined to describe the link between electromagnetic wavelength distributions in the visible spectrum, and physiologically perceived colors in human color vision. The CIE 1931 RGB color space and CIE 1931 XYZ (tristimuli) color space were created by the CIE as a result of a collection of studies done by W.D. Wright²² and J. Guild²³.

The tristimulus X , Y , Z that define the color of the transmitted beam are given by the following integrals^{24,25},

$$X = \int_{\lambda_1}^{\lambda_2} S(\lambda) G(\lambda) \bar{x}_\lambda d\lambda \\ Y = \int_{\lambda_1}^{\lambda_2} S(\lambda) G(\lambda) \bar{y}_\lambda d\lambda \\ Z = \int_{\lambda_1}^{\lambda_2} S(\lambda) G(\lambda) \bar{z}_\lambda d\lambda \\ (20)$$

where $S(\lambda)$ is the spectral distribution of the source, $G(\lambda)$ is the transmission of the considered filter, \bar{x}_λ , \bar{y}_λ and \bar{z}_λ are the three sensitivity functions of the human eye (CIE 1931), and λ_1 , λ_2 represent the spectrum interval in which the receiver is sensitive, that in the human eye case, evaluates a wavelength range approximately of [400, 700] nm.

If the XYZ space is determined, the RGB channels can be calculated through the following linear transformation^{26,27},

$$\begin{pmatrix} R \\ G \\ B \end{pmatrix} = \begin{pmatrix} 0.419 & -0.159 & -0.083 \\ -0.091 & 0.252 & 0.016 \\ 0.001 & -0.003 & 0.179 \end{pmatrix} \begin{pmatrix} X \\ Y \\ Z \end{pmatrix} \\ (21)$$

3. POLARIZATION APPLET

In this section, we provide a brief description of the different polarization educational utilities and the tools included in the polarization applet, which are devoted to train the polarization concepts described in section 2. This section is structured in diverse subsections, where in each one some particular polarization concepts are gathered. In fact, each one of the subsections is related to a particular polarization applet tab, as the software is also organized by sorting different polarization topics.

The main screen (see Fig. 3) is divided in different sectors. In the left part, there are several tabs with the operations that can be performed in the polarization applet. In the right part, the graphical representations of the results are displayed. On the bottom left two different buttons allow to clean graphs and to stop the program, respectively.

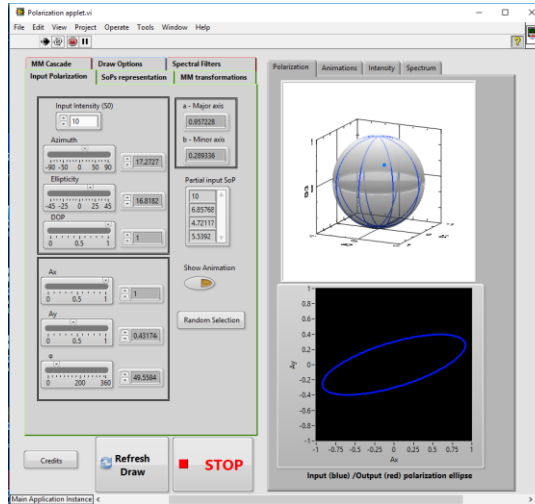


Figure 3. Main screen of the polarization applet.

3.1 States of polarization generation and representation

Starting from the main menu, the options to generate arbitrary states of polarization (SoP) and see different SoPs representations (ellipse of polarization and Poincaré sphere) are found in the “Input Polarization” tab (see Fig. 4(a)).

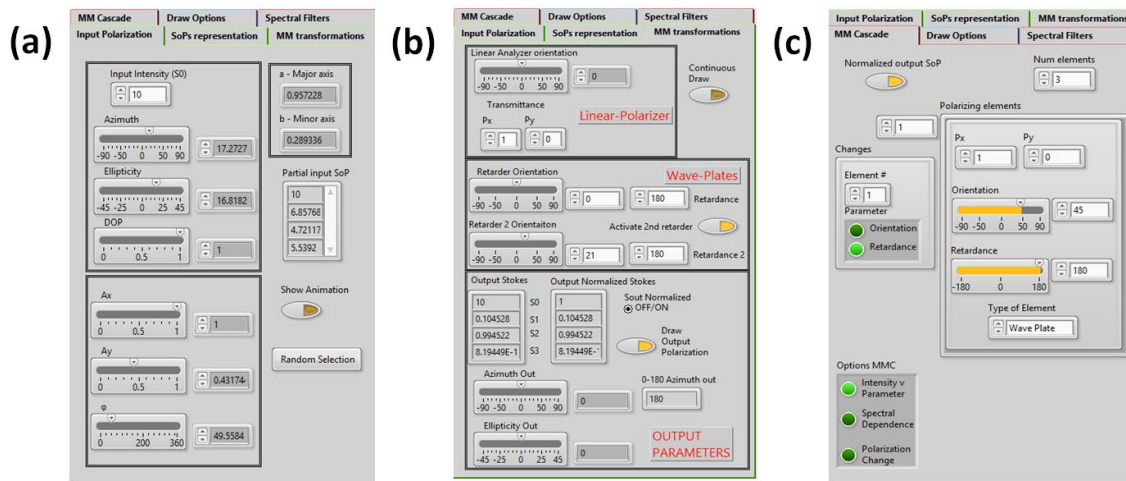


Figure 4. (a) Input Polarization tab; (b) MM transformations tab; and (c) MM Cascade tab.

There are several options to specify the polarization state:

- By means of the polarization ellipse parameters: azimuth, ellipticity, and intensity. For partially polarized light, the Degree of Polarization (DoP) can also be changed.

- By means of the amplitude components (A_x, A_y) and the phase shift (φ) between them.
- By pressing the button “Random Selection” a random polarization state is generated.

If some parameter is changed in one of these representations, the parameters in the other representations are changed automatically, in order to show the corresponding equivalence. Finally, the major and minor axes of the polarization ellipse and the Stokes representation are evaluated.

In the representation side (right side of the main container), we found the “Polarization” tab, in which the polarization ellipse corresponding to the selected polarization state (fully polarized) is drawn. In addition, the corresponding Stokes vector is plotted over the Poincaré sphere, being represented by a blue dot (see Fig. 3).

If the button “Show Animation” is at the ON mode, the “Animation” tab in the representation side is activated. In that case, an animation of the polarization ellipse and the wave propagation are represented, in which the 3D draw of the vibrating field propagation can be spatially rotated for a better visualization.

3.2 Polarization transformations

The Stokes vector evaluated in the previous section, and written in the vector “Partial input SoP” in the “Input Polarization” tab, it is used as the input polarization for the polarization transformations which are subject of discussion in this subsection. In order to study the interaction of light with matter in the basis of the Stokes-Mueller formalism (see sections 2.1 and 2.2), the “MM transformations” tab, shown in Fig. 4(b), allows users to transform the input polarization state by two different polarizing elements: (i) a polarizer; and (ii) one or two linear retarders. In the latter case, the default mode evaluates the interaction of the input polarization with one linear retarder, but by clicking the “Activate 2nd retarder” button (Fig. 4(b)), the applet provides the interaction of light with two arbitrary linear retarders in cascade. The applet allows users choosing the transmission axis of the polarizer and its transmittance values, and the retardance and neutral lines orientation for the retarders. Therefore, a wide range of scenarios can be simulated.

The polarization data after interaction with the different polarization elements selected (i.e., the characteristics of the output polarization) is written at the bottom of this tab (see Fig. 4(b)). In particular, the output Stokes vector, the output normalized Stokes vector, and the azimuth and ellipticity angles of the output ellipse of polarization (for the fully polarized contribution) are provided. What is more, the output polarization ellipse is displayed in red in the tab “Polarization”, superimposed to the input ellipse of polarization, which is represented in blue (see Fig. 5(a)). In addition, the output Stokes is also displayed over the Poincaré Sphere. If the button “Continuous Draw” is in the ON mode, the history of the output polarization is drawn in the Poincaré sphere (see an example in Fig. 5(b)).

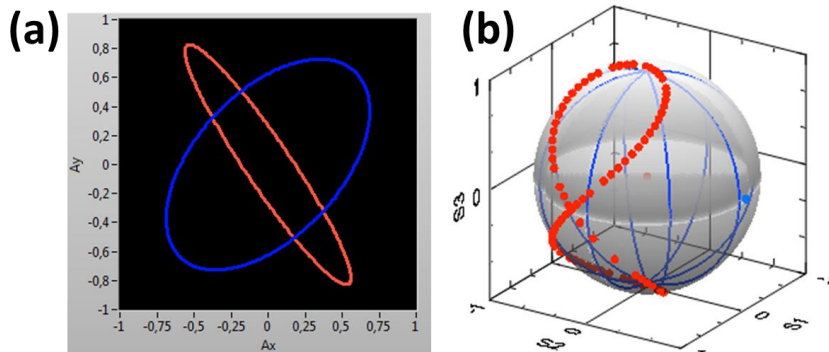


Figure 5 (a) Polarization ellipse for the input (blue) and output (after transformation; in red) states; (b) Poincaré sphere with the history of a collection of transformations (rotating quarter-waveplate for an input linear polarization oriented at 45°).

Another virtual space in the applet whose content is also focused on polarization transformations is the “MM Cascade” tab (see Fig. 4(c)), in which a generalization of the polarization-matter interactions discussed in the “MM transformations” tab is provided. In particular, in the “MM Cascade” tab the input polarization can be transformed by customized series of polarizing elements. The number of elements can be chosen, and for each element in the series, we select between a linear polarizer or a retarder. For each element we have to choose: (i) whether it is a polarizer or a retarder; (ii) the transmission of each axis (P_x, P_y) and their orientation (in the case of a polarizer); and (iii) the orientation of the neutral lines and the retardance.

After calculating the output polarization corresponding to the customized polarizing elements cascade, the particular data of the output polarization is obtained and some representations can be shown. In particular, at the left-bottom corner of the “MM Cascade” tab we found the “Options MMC” button, where three main options can be selected,

3.2.1 Intensity vs parameter

By choosing this option, we can study the intensity (S_0 stokes channel) at the exit of the customized cascade as a function of some parameter of interest corresponding to a specific polarizing element in the cascade. In particular, in the box “Changes” we have to choose the specific optical element to be studied (“number #” box), and the parameter to change (orientation or retardance). The output intensity corresponding to the values selected is then displayed (see Fig. 6(a)).

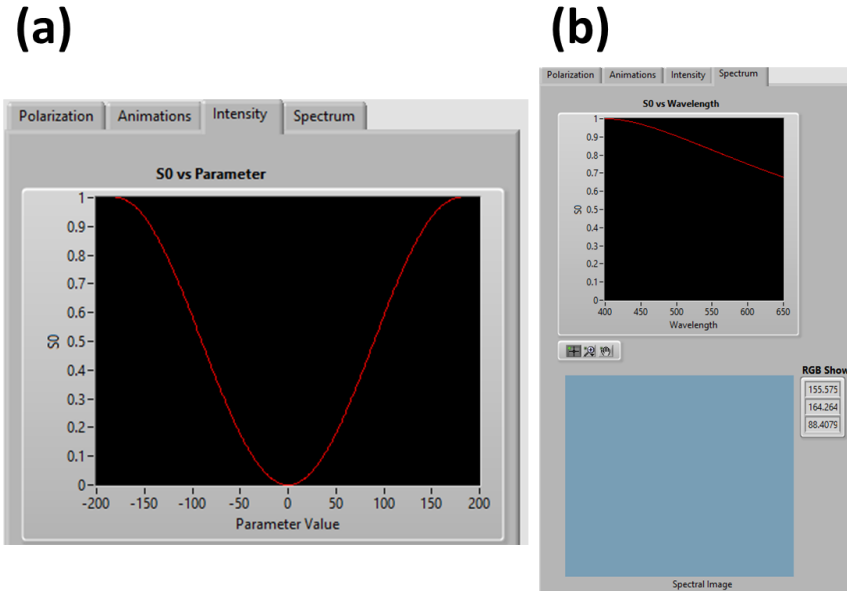


Figure 6 (a) Intensity vs Parameter (orientation or retardance) value; and (b) output intensity versus wavelength and color image of the output beam displayed in the Spectrum tab.

3.2.2. Spectral dependence

By selecting the “Spectral dependence” option in the “Options MMC” button, the applet conducts a representation of the observed color at the exit of the optical filter corresponding to the designed polarizing elements cascade. The applet calculations are based on the mathematical description shown in section 2.3.3, but some extra assumptions are made. First, we are assuming that the input light beam is polychromatic with a constant intensity in all the spectral range. The studied spectral range is controlled by the “ini wavelength” and “final wavelength” boxes that can be modified by users, these boxes only appearing if selecting the radiobutton “Spectral Dependence” (this is why they do not appear in Fig. 4(c), where the “Intensity v Parameter” is selected”). The second assumption is that the refraction indices of the retarders in the cascade do not depend on the wavelength, and the only dependence of the retardance with the wavelength is due to the light wavenumber. Therefore, the relation between the retardance corresponding to the first wavelength in the selected spectrum with the retardance for the i th wavelength is obtained by,

$$\delta(\lambda) = \frac{2\pi}{\lambda} (\Delta n) d \Rightarrow \frac{\delta(\lambda_i)}{\delta(\lambda_1)} = \frac{\lambda_i}{\lambda_1} \Rightarrow \delta(\lambda_i) = \delta(\lambda_1) \frac{\lambda_i}{\lambda_1} \quad (22)$$

where $\Delta n = n_e - n_o$ is the difference between the extraordinary and ordinary indices of refraction.

As the transmission could be very low, the output intensities are multiplied by a factor that can be selected by the user. According to the description in section 2.3.3, the *RGB* channels are obtained for a particular cascade configuration customized by users, and the output intensity versus the wavelength and the color of the output beam are displayed in the corresponding figures at the Spectrum tab (see an example in Fig. 6(b)).

3.2.3. Polarization change

By selecting the “Polarization Change” option in the “Options MMC” button (see Fig. 4(c)), the polarization of the output beam is calculated and displayed in the corresponding figures. Note that you can set to ON mode the button “Continuous Draw”, and then, the history of the polarizations is displayed on the Poincaré sphere.

3.3 Spectral filters

The same spectral dependence concept discussed in the applet “MM cascade” tab is studied in the “Spectral Filters” tab (see Fig. 7). However, two particular schemes, corresponding to two well-known polarizing filters (the Lyot filter and the Solc filter), are set this time. The optical schemes of these two filters are discussed in section 2.3. The applet allows users to modify some characteristic parameters of the filters, and to study the corresponding output intensity versus the wavelength and the color of the output beam. This information is displayed for each new modification of the filter in the corresponding figures at the Spectrum tab. In this way, we can study, in a dynamic and very intuitive way, some important properties of the intensity distribution of the filter (as the number or the bandwidth of the intensity peaks) as well as the final visual sensation (color at the exit of the filter), all of this as a function of the parameters of interest.

In the case of the Lyot filters (Fig. 7(a)), a linear analyzer is always set at the end of the cascade, and the user can modify the number of polarization-waveplate blocks, the orientation of the linear analyzer, the orientation of the retarders (all of them share the same orientation), and their retardance (all share the same retardance). The optical parameters involved in the waveplate retardance, as the thickness, the ordinary and extraordinary indices can also be customized by the user. In such a way, the applet can be used as well to model possible implementations of Lyot filters based on real anisotropic uniaxial materials, as those based on quartz and calcite crystals with different thicknesses.

By turn, in the case of Solc filters (Fig. 7(b)), the input and output linear polarizers are set at 0° of the laboratory vertical, and some parameters of the N retarders sandwiched between the polarizers can be controlled by users. In this regard, we can modify the number of waveplates and their retardance. As in the Lyot filter case, some waveplate physical parameters related to the retardance, as the thickness, or the ordinary and extraordinary indices, can also be customized by the user. What is more, in regard to the waveplates orientation, the software allows multiple possibilities to tune the angular distribution of the plates. The user must set the initial orientation angle (i.e., the orientation among the first polarizer and the first retarder), and from this initial value, some angular functions can be chosen, as a linear variation of the angle between plates, or some non-linear functions, as trigonometric, exponential or Gaussian angular functions, among others. In all the cases, the corresponding graphical visualizations (intensity distribution and final color) are provided, in order to study the effect of the different parameters of interest in the filter performance.

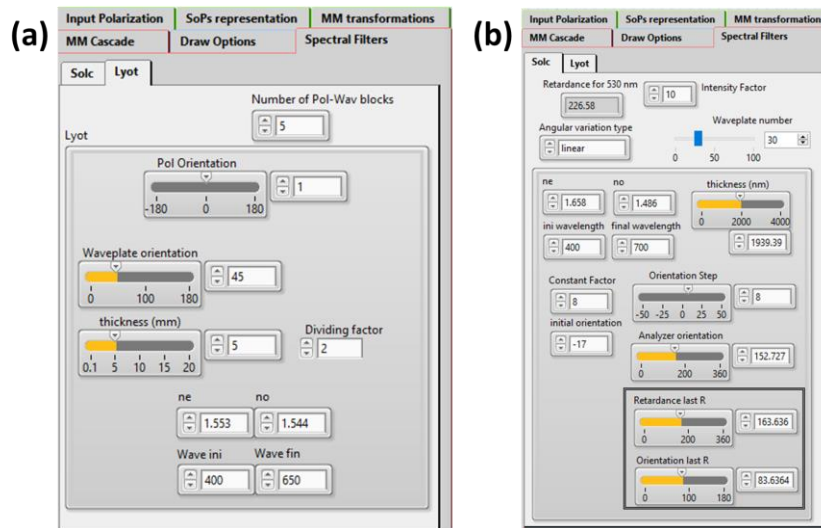


Figure 7 (a) Lyot filter control panel; and (b) Solc filter control panel.

4. POLARIZATION TRAINING BY USING THE VIRTUAL ENVIRONMENT: USER-POLARIZATION APPLET INTERACTION

There are multiple approaches that can be used to train students with the help of a virtual applet. The interest of using educational applets to train mathematic and scientific concepts has been already discussed in literature^{28,29}. It is known how, by using applets, it is possible to generate multiple and dynamic examples, increasing the potential of a single image, without loss of space. Interactive applets allow teachers to perform tailored exercises to be solved by students, to get feedback of their understanding with regard to some definitions and concepts or to promote a line of scientific reasoning according to a series of steps that students must follow through some applet functionalities. They also arise as an ideal platform for on-line lessons and give access to scientific experiments into a virtual environment, this being of special interest in educational institutions where real experimental facilities are not available.

In this section, we briefly describe the specific approximation we have used to train, through the applet gadgets provided in section 3, the polarization concepts explained in section 2.

The educational method was devised to be applied with students attending the Optics course of the Physics degree in the Universitat Autònoma de Barcelona (UAB). In the Optics course, a mandatory subject taught at the third year of the Physics degree, the optics fundamentals are described in detail: geometrical optics, waves, polarization, dispersive materials, anisotropy, interferences and diffraction. The applet being subject of discussion in this manuscript focus on reinforcing the students' knowledge related to the polarization block.

The educational approach we use to train polarization through the polarization applet consists of the following main steps:

- (1) Theoretical concepts are provided through theoretical classes. The main polarization concepts provided are those summarized in section 2.
- (2) The students play with the applet to get familiar with the environment and possibilities. They can download an executable of the applet through the Virtual Campus of the UAB, an online learning focused on the learning process. By accessing to the Optics course in the Virtual Campus, different supporting tools and notes are accessible, being the polarizing applet one of them. Once they have downloaded the applet, they can install it to their computers and get familiar with the different menu tabs, and the polarization tools and graphics into them. An instruction manual of the applet is also accessible via Virtual Campus material. The LabView Run-Time engine installer is the only requirement to run the applet, and can be freely downloaded from the National instruments webpage.
- (3) Some questions are set by teachers, which can only be solved by using the applet. The purpose of these questions is twofold. On the one hand, they are related to some concepts described in section 2, and that have to be investigated through some applet tools, and analyzed via some graphical representations. In this way, students can easily link mathematical relations in section 2, with visual representations of physical phenomena, and to study the dependence of some parameters of equations in section 2, with modifications in the visual representations of those phenomena (i.e., changes in the polarization ellipse, the final position of the Stokes vector in the Poincaré sphere, modifications of the intensity distribution at the exit of a polarizing element cascade, the color image at the exit of a polarizing filter, etc.). In addition, different tabs are related to different knowledge levels, so polarization concepts can be progressively taught by selecting a collection of questions specific of a particular educational block (i.e., specific questions for each different tab in the applet). On the other hand, by solving the questions, students are not only reinforcing their knowledge but they are also giving us feedback of how they are assuming some polarizing concepts. In fact, answers give us information of where they are having learning problems and in which concepts teachers must focus, or use different approaches, so that students achieve a deep learning of the subject matter.
- (4) A discussion of the obtained results and answers provided by students is conducted to better link theory with virtual data and the experiences conducted.

For the sake of example, some questions that can be asked in order to take profit of the applet for polarization training are provided in the following:

- i) Generate a linear polarization state with a given azimuth. In the tab "MM transformations": (a) select the retardance of the wave plate (for instance 90°); (b) change the Retarder Orientation and NOTE that when it coincides with the azimuth

or perpendicular to the azimuth the output polarization state is the same as the input one. Note that at these orientations the output polarization state is independent of the wave-plate retardance (change the retardance).

ii) Demonstrate that two half waveplates act as a polarization rotator of an angle equal to twice the angle between both. Use the polarization applet to visualize this. First select an input polarization state in the tab “Input Polarization”, then, in the tab “MMtransformations”, set the retardance of both wave-plates to 180° , select the button “Activate 2nd retarder” and change the Orientation of one of the retarders. You will visualize the output Stokes, Azimuth, and ellipticity, and you can see the polarization ellipse and the Poincaré sphere. If the button “Continuous Draw” is ON, then you can see the evolution of the output polarization state. Does the Ellipticity change?

iii) Demonstrate that with a linear polarizer at 0° and two variable wave-plates with arbitrary retardance, oriented at 45° and at 0° respectively, it is possible to obtain any fully polarized state of polarization. What are the retardances needed to obtain a given Stokes vector? NOTE that the retardances solution is not unique when the waveplates retardation range is $[0-2\pi]$.

Use the tab “MM transformations”, set the retarder orientations, set the “activate de 2nd retarder” button to ON and the “Continuous Draw”. Change the retardance of the first retarder gradually until arriving to the desired retardance, and then make the same with the second retarder to visualize the trajectory of the polarization on the Poincaré sphere. Try to obtain the following output polarization states:

a) Linear polarization at 45° , linear polarization at 22.5° , (and other linear ones). Note that in this case, in one of the solutions, the retardance of the first retarder should be twice the final azimuth, and the retardance of the second retarder should be 90° .

b) Some elliptical polarizations. What combination of optical elements have you used to achieve such state?

iv) Let us assume that we have a linear polarizer and a wave plate. How can we obtain circularly polarized light? Is it possible to obtain it with arbitrary retardance of the waveplate? Show this with the applet.

v) Let us assume we have a linear polarizer and a variable wave-plate that we can rotate. Is it possible to obtain any polarization state? If yes, what should be the orientation of both devices and retardance of the wave-plate? Implement this in the Polarization applet.

vi) Let us assume that we have two linear polarizers and a quarter-wave plate, but we do not know the location of the respective axes. Can we measure the light intensity but not its polarization? Describe a method to obtain circularly polarized light. Implement it in the polarization applet.

vii) A quarter waveplate is rotated between two crossed Polaroids. If an unpolarized beam is incident on the first Polaroid, discuss the variation of intensity of the emergent beam as the quarter waveplate is rotated. What will happen if we have a half waveplate instead of a quarter wave plate?

viii) (a) Consider two crossed Polaroids placed in the path of an unpolarized beam of intensity I_0 . If we place a third Polaroid in between the two, then, in general, some light will be transmitted through. Explain this phenomenon. (b) Assuming the pass axis of the third Polaroid to be at 45° to the pass axis of either of the Polaroids, calculate the intensity of the transmitted beam. Assume that all the Polaroids are perfect.

ix) Consider we have two crossed polarizers and a variable waveplate between them. (a) Evaluate the output irradiance as a function of the retardance. (b) What should be the waveplate orientation to obtain the maximum contrast? (c) Implement this set-up in the polarization applet.

5. CONCLUSIONS

In this manuscript we have discussed the interest of using a virtual environment to teach polarization concepts to students at different educational levels. In particular, a polarization applet was developed that includes different polarization fundamentals, as the polarization ellipse, the Stokes vectors, the Poincaré sphere representation, the Mueller matrix of a sample, the cascade of Mueller matrices, polarizing filters, among others.

The applet is organized in a way that related polarization concepts are gathered together in the same tab. What is more, polarization concepts of different levels are sorted in different tabs. In particular, students have access to the following tabs: (i) “Input Polarization” tab, where different descriptions of polarization states (fully or partially polarized) are

shown, (ii) to the “MM transformation” tab, where polarization-matter interactions are studied, (iii) “MM cascade” tab, in which the effect of a customized cascade of polarizing elements on an input polarization is analyzed and (iv) “Spectral Filters”, in which two well-known polarization filters (Lyot and Solc filters) are inspected. In all the cases, the user has control to different physical parameters involved, that can be dynamically modified, and results are represented in different formats and spaces. The mathematical background of the polarization concepts included in the applet were provided in section 2, and a description of the different tabs above stated was given in section 3. A discussion about the educational approach used to teach polarization through the virtual environment of the applet was provided in section 4.

To promote an efficient students-applet interaction, we also include in the training methodology a collection of leading questions that students must answer with the help of the applet. A list of questions that can be used to teach polarization through the applet functionalities were also provided in this manuscript.

The use of a polarization applet provides some educational advantages. It allows generating multiple and dynamic examples. It allows us to perform tailored exercises to be solved by students, reinforcing what they learned in theoretical sessions. What is more, it gives access to scientific experiments into a virtual environment, this being of special interest in educational institutions where real experimental facilities are not available. The applet environment can be used in several ways: (a) in interactive sessions with the teacher in class, (b) proposing practical questions that the student must solve at home (like those proposed in section 4), (c) it also permits advanced students to self-learning at home.

ACKNOWLEDGMENTS

We acknowledge the financial support of Spanish MINECO (FIS2015-66328-C3-1-R, and Fondos FEDER); Catalan Government (SGR 2014-1639).

REFERENCES

- [1] M. Born and E. Wolf, [Principles of Optics: Electromagnetic Theory of Propagation, Interference and Diffraction of Light], 7th edition, Cambridge University Press (1999).
- [2] R.M.A. Azzam and N.M. Bashara, Ellipsometry and Polarized Light, (North-Holland Publishing Company, 1977).
- [3] V.A. Escobar, J.R. Rangel, N.V. Pérez, G. Andrade, and J.L. Dávila, Infrared Spectroscopy – Materials Science, Engineering and Technology, (Intech, 2012), Chap. 9.
- [4] N.L. Do, E. Garcia-Caurel, N. Bererd, N. Moncoffre, and D. Gorse-Pomonti “Determination of thicknesses of oxide films grown on titanium under argon irradiation by spectroscopic ellipsometry,” J. Nucl. Mater. 447 (1-3), 197-207 (2014).
- [5] A. Lizana, M. Foldyna, M. Stchakovský, B. Georges, N. David, and E. Garcia-Caurel, “Enhanced sensitivity to dielectric function and thickness of absorbing thin film by combining total internal reflection ellipsometry with standard ellipsometry and reflectometry,” J. Phys. D: Appl. Phys. 46(10), 105501 (2013).
- [6] S.R. Cloude, [Polarization: Applications in Remote Sensing], Oxford University Press, 1-446 (2010).
- [7] N. Uribe-Patarroyo, A. Alvarez-Herrero, R.L. Heredero, J.C. del Toro, A.C. López, V. Domingo, J.L. Gasent, L. Jochum, and V. Martínez, “IMaX: a polarimeter based on liquid crystal variable retarders for an aerospace mission,” Phys. Status Solidi C 5, 1041-1045 (2008).
- [8] D.F. Elmore, B.W. Lites, S. Tomeczyk, A. Skumanich, R.B. Dunn, J.A. Schuenke, K.V. Streander, T.W. Leach, C.W. Chambellan, H.K. Hull, and L.B. Lacey, “Advanced Stokes polarimeter: a new instrument for solar magnetic field research”, Proc. SPIE 1746, 138795 (1992).
- [9] K. M. Twietmeyer, R.A. Chipman, A.E. Elsner, Y. Zhao, and D. VanNasdale, “Mueller matrix retinal imager with optimized polarization conditions,” Opt. Exp. 16(26), 21339 (2008).
- [10] M.R. Antonelli, A. Pierangelo, T. Novikova, P. Validire, A. Benali, B. Gayet, and A. De Martino, “Mueller matrix imaging of human colon tissue for cancer diagnostics: how Monte Carlo modeling can help in the interpretation of experimental data,” Opt. Exp. 18(10), 10200-10208 (2010).
- [11] X. Feng, R. Patel, and A.N. Yaroslavsky, “Wavelength optimized cross-polarized wide-field imaging for noninvasive and rapid evaluation of dermal structures”, Journal of Biophotonics, 8(4), 324-331 (2015).

- [12] V.V. Tuchin, L. Wang, D.A. Zimnyakov, [Optical polarization in biomedical applications], Springer Science & Business Media (2006).
- [13] I. Meglinski, C. Macdonald, A. Doronin, B. Kunnen, and M. Eccle “Polarized Light Biosensing”, Asia Communications and Photonics Conference papers, Optical Society of America, ATh2G-2 (2014).
- [14] A. Van Eeckhout, A. Lizana, E. Garcia-Caurel, J.J. Gil, A. Sansa, C. Rodríguez, I. Estévez, E. González, J.C. Escalera, I. Moreno, and J Campos, “Polarimetric imaging of biological tissues based on the indices of polarimetric purity”, *J. of Biophotonics* 11(14), e201700189 (2018).
- [15] A. Van Eeckhout , E. Garcia-Caurel, T. Garnatje, M. Durfort, J.C. Escalera, J. Vidal, J.J. Gil, J. Campos, A. Lizana, “Depolarizing metrics for plant samples imaging”, *PLOS ONE* 14(3), e0213909 (2019).
- [16] Ch. Patty, D. Luo, F. Snik, F. Ariese, W.J. Buma, K. Ten, R.J.M Van Spanning, W.B. Sparks, T. Germer, G. Garab, M.W. Kudenov, “Imaging linear and circular polarization features in leaves with complete Mueller matrix polarimetry”, *Biochim. Biophys. Acta Gen. Subj.* 1862(6), 1350-1363 (2018).
- [17] D. Goldstein, [Polarized light], Marcel Dekker, New York (2013).
- [18] B. Lyot, “Le filtre monochromatique polarisant et ses applications en physique solaire”, *Ann. Astrophys.* 7, 31 (1944).
- [19] I. Solc, “A new type of filter”, *Czechoslovak Journal of Physics*, 4(1) 95-118 (1953).
- [20] J.W. Evans, “Solc Birefringent Filter”, *J. Opt. Soc. Am.* 48(3), 142-145 (1958).
- [21] S.E. Harris, E.O. Ammann, I.C. Chang, “Optical Network Synthesis Using Birefringent Crystals. I. Synthesis of Lossless Networks of Equal-Length Crystals”, *J. Opt. Soc. Am.* 54(10), (1964).
- [22] W.D. Wright, “A re-determination of the trichromatic coefficients of the spectral colors”, *Trans. Opt. Soc.* 30 (4), 141–164. (1929).
- [23] J. Guild, “The colorimetric properties of the spectrum”, *Phil. Trans. R. Soc. A* 230, 149–187(1932).
- [24] G. Wyszecki and W. S. Stiles, *Color Science*, John Wiley, New York (1970).
- [25] J. Casas, [Optica], 7 edition, Librería Pons, Zaragoza (1994).
- [26] H.S. Fairman, M.H. Brill, H. Hemmendinger, “How the CIE 1931 Color-Matching Functions Were Derived from the Wright–Guild Data” *Color Res. Appl.* 22(1), 11–23(1997).
- [27] H.S. Fairman, M.H. Brill, H. Hemmendinger, “Erratum: How the CIE 1931 Color-Matching Functions Were Derived from the Wright–Guild Data”, *Color Res. Appl.* 23 (4): 259–259 (1998).
- [28] C.P. Mawata, “Uses of Java Applets in Mathematics Education”, *Asian Technology Conference in Mathematics (ATCM)*, (1998).
- [29] F. Al-Zahrani, “Web-Based Learning and Training for Virtual Metrology Lab”, *J. Telecommun.* 1(2), 42-54 (2010).